sciendo

Int. J. Appl. Math. Comput. Sci., 2020, Vol. 30, No. 2, 337–350
DOI: 10.34768/amcs-2020-0026

amcs

DEFORMED SOLITONS OF A TYPICAL SET OF (2+1)–DIMENSIONAL COMPLEX MODIFIED KORTEWEG–DE VRIES EQUATIONS

FENG YUAN [a], XIAOMING ZHU [a], YULEI WANG [b,*]

[a] School of Mathematical Sciences
University of Science and Technology of China
Hefei, Anhui 230026, PR China

[b] Department of Engineering and Applied Physics
University of Science and Technology of China
Hefei, Anhui 230026, PR China
e-mail: wyulei@ustc.edu.cn

Deformed soliton solutions are studied in a typical set of (2+1)-dimensional complex modified Korteweg–de Vries (cmKdV) equations. Through constructing the determinant form of the n-fold Darboux transformation for these (2+1)-dimensional cmKdV equations, we obtain general order-n deformed soliton solutions using zero seeds. With no loss of generality, we focus on order-1 and order-2 deformed solitons. Three types of order-1 deformed solitons, namely, the polynomial type, the trigonometric type, and the hyperbolic type, are derived. Meanwhile, their dynamical behaviors, including amplitude, velocity, direction, periodicity, and symmetry, are also investigated in detail. In particular, the formulas of $|q^{[1]}|$ and trajectories are provided analytically, which are involved by an arbitrary smooth function $f(y + 4\lambda^2 t)$. For order-2 cases, we obtain the general analytical expressions of deformed solitons. Two typical solitons, possessing different properties in temporal symmetry, are discussed.

Keywords: (2+1)-dimensional complex modified Korteweg–de Vries equation, Darboux transformation, deformed soliton solution.

1. Introduction

Integrable systems, constructing and studying nonlinear partial differential equations (NPDEs) describing natural phenomena, have significant influence on both mathematical and physical fields. In recent years, nonlinear science has been highly developed and widely applied in many areas such as hydrodynamics, plasma physics, marine science, and optical fiber communication. The earliest research on integrable systems can be traced back to the Scottish scientist John Scott Russell, who observed solitary waves in 1834 (Russell, 1844). After six decades, Korteweg and de Vries developed a mathematical model, namely, the Korteweg–de Vries (KdV) equation, to describe the aforementioned water wave, which helped to prove the existence of solitary waves (Korteweg and de-Vries, 1895). In the mid-1960s, Zabusky and Kruskal discovered the remarkably stable particle-like behavior of solitary waves (Zabusky and Kruskal, 1965). According to their work, solitary waves described by the KdV equation can pass through each other keeping their speed and shape unchanged. As a result, the name "soliton" is defined. In the wake of these discoveries, solitary wave theory boosted the development of many areas of science and technology. After one hundred years, integrable systems developed deeply and soliton theory was widely applied in many areas (Ablowitz *et al.*, 1991). Up to now, soliton solutions have been found in hundreds of NPDEs, some of which have been discovered in experiments (Ablowitz *et al.*, 1991; Mollenauer *et al.*, 1980).

Through the Miura transformation, the KdV equation can lead to the famous modified Korteweg–de Vries (mKdV) equation, which is expressed as

$$q_t + 6q^2 q_x + q_{xxx} = 0. \tag{1}$$

It is applied well in dynamical systems, fluid mechanics,

*Corresponding author

plasma physics and other physical fields (Komatsu and Sasa, 1995; Lonngren, 1998; Khater *et al*., 1998). The mKdV equation has been studied by the inverse scattering transformation (Wadati, 1972; 2008; Wadati and Ohkuma, 1982; E-Tantawy and Moslem, 2014), the Hirota bilinear method (Hirota, 1972), and the Darboux transformation (Wu *et al.*, 2008; Xu *et al.*, 2011; Xing *et al.*, 2017a; 2017b). The Darboux transformation (DT), which can construct new solutions from a trivial seed, has been studied deeply to find new analytical solutions for many NPDEs (Zhang *et al.*, 2015; 2017).

After being generalized to the complex field, the mKdV (1) forms the famous complex modified Korteweg–de Vries (cmKdV) equation, namely,

$$q_t + q_{xxx} + \alpha|q|^2 q_x = 0. \tag{2}$$

This equation has been applied widely, e.g., in the molecular chain model, the generalized elastic solid, and so on (Gorbacheva and Ostrovsky, 1983; Erbay and Şuhubi, 1989; Erbay, 1998; Zha and Li, 2008; He *et al*., 2014; Yan and Zheng, 2017). Especially, the cmKdV equation shows its ability in construction of magnetic confined fusion devices. Nonlinear interactions between low-hybrid waves and plasmas can be described well by using the cmKdV equation (Karney *et al*., 1979).

The development history of KdV systems implies that mathematical generalization of nonlinear equations can provide powerful theoretical support for physical and experimental discoveries. Among all the generalization ways, ascending dimensions of integrable systems is an elegant one. Through extra variables, spatial dimensions of nonlinear equations can be added, but the basic properties of the original equations remain, which is vital for analysis. In the cmKdV case, to study their usage in applied magnetism and nanophysics, it has been generalized to (2+1)-dimensions (Myrzakulov *et al*., 2015). One typical form of the (2+1)-dimensional cmKdV equation is

$$\begin{cases} q_t + q_{xxy} + (qw)_x + iqv = 0, \\ v_x + 2i(q_{xy}q^* - qq^*_{xy}) = 0, \\ w_x - 2(|q|^2)_y = 0. \end{cases} \tag{3}$$

The corresponding Lax pair is

$$\Psi_x = A\Psi, \quad \Psi_t = 4\lambda^2\Psi_y + B\Psi, \tag{4}$$

with

$$A = \lambda J + A_0, \quad B = \lambda B_1 + B_0,$$
$$\Psi = \begin{bmatrix} \psi_1(\lambda, x, y, t) \\ \psi_2(\lambda, x, y, t) \end{bmatrix}, \quad J = \begin{bmatrix} -i & 0 \\ 0 & i \end{bmatrix},$$
$$B_0 = \begin{bmatrix} -\frac{iv}{2} & -q_{xy} - wq \\ r_{xy} + wr & \frac{iv}{2} \end{bmatrix},$$
$$A_0 = \begin{bmatrix} 0 & q \\ -r & 0 \end{bmatrix}, \quad B_1 = \begin{bmatrix} iw & 2iq_y \\ 2ir_y & -iw \end{bmatrix},$$

where $r = q^*$, $\lambda \in \mathbb{C}$, and "*" is the conjugation operator, while v and w are real functions that denote the scalar potential fields interacting with the spin field (Myrzakulov *et al*., 2015). The usage of v and w can also simplify the calculations of the (2+1)-dimensional cmKdV equation. Further, Ψ is the eigenfunction of the spectral problem (4) corresponding to the eigenvalue λ. Order-1 and order-2 regular solitons of this equation have been deduced by using the two-fold Darboux transformation (Yesmakhanova *et al*., 2017). In this paper, however, we step forward and focus on deformed soliton solutions.

In contrast to regular solitons traveling with constant speed and shape, deformed solitons show quite sophisticated behaviors, which possess temporal changeable speed and might transform their shapes during evolution. For NPDEs with variable coefficients, fruitful deformed solitons have been discovered. Dai *et al*. (2010) or Sun and Yu (2011) construct shape-changing soliton solutions with variable speed, and trigonometric type solitons have also been found in Lü *et al*. (2007), Pal *et al*. (2017) or Osman and Wazwaz (2018). Meanwhile, for NPDEs with constant coefficients, many works have been published on the topic of deformed solitons. In a (1+1)-dimensional Hirota equation, the effects of soliton interactions on the formation of deformed phenomena are discussed (see He *et al*., 2013). Porsezian *et al*. (2006), Kundu (2008), Tao and Porsezian (2013), Li *et al*. (2013) and Liu *et al*. (2015) construct deformed soliton solutions. For the (2+1)-dimensional equation, Biondini (2007), Kodama *et al*. (2009) or Kao and Kodama (2012) give the deformed solitons of KPI and KPII equations, while Zhang and Xue (2009) construct a parabolic soliton of a (2+1)-dimensional NLS equation. In this paper, considering the attention paid to deformed solitons in different types of NPDEs, we will look for deformed soliton solutions with different orders for Eqn. (3). The fundamental method we use is the N-fold Darboux transformation. Dynamical behaviors of order-1 and order-2 deformed solitons will be analyzed in detail.

This paper is organized as follows. In Section 2, we give the determinant form of the n-fold Darboux transformation (DT) and the order-n soliton solutions of the (2+1)-D cmKdV equation (3). In Section 3, we study in detail three types of order-1 deformed soliton solutions: the polynomial type soliton, trigonometric type soliton, and hyperbolic type soliton. Their formulas, trajectories, and figures are provided. In Section 4, we study order-2 deformed solitons and analyze their dynamical behaviors.

It is worth noting that we can obtain mixed-type deformed solitons in high-order cases. In Section 5, we conclude this paper.

2. Darboux transformation and order-n solutions

The Darboux transformation is a gauge transformation which can keep the form of the spectral problem unchanged. The main assignment in this section is to present the determinant representation of the n-fold transformation and n-order solutions for the (2+1)-D cmKdV equation. First, we need to find a 2×2 matrix T_n so that the spectral problem (4) is covariant, and then obtain a new solution $(q^{[n]}, w^{[n]}, v^{[n]})$ expressed by the elements of T_n and the seed solution (q, w, v). Next, we need to find the expressions of the elements of T_n in terms of the eigenfunctions of the spectral problem corresponding to the seed solution (q, w, v).

Then we need to obtain the determinant representation of the n-fold DT T_n and new solutions $(q^{[n]}, w^{[n]}, v^{[n]})$. The 1-fold and 2-fold Darboux transformations of the (2+1)-D cmKdV equation (3) were obtained by Yesmakhanova *et al*. (2017). In this paper, we suppose the Darboux matrix T_n is in the form

$$T_n = D_0 + \lambda D_1 + \cdots + \lambda^{n-1} D_{n-1} + \lambda^n I, \quad (5)$$

where T_n and $D_j (j = 0, \ldots, n-1)$ are 2×2 matrices and I is the identity matrix. First, we introduce n eigenfunctions Ψ_j as

$$\Psi_j = \begin{bmatrix} \psi_{j1}(\lambda_j, x, y, t) \\ \psi_{j2}(\lambda_j, x, y, t) \end{bmatrix}, \quad j = 1, \ldots, n.$$

From the algebraic equation

$$\Psi_j^{[n]} = T_n(\lambda; \lambda_1, \lambda_2, \cdots, \lambda_n)|_{\lambda=\lambda_j}\Psi_j = 0 \quad (6)$$

we can obtain the determinant representation of T_n.

Theorem 1. *The n-fold Darboux transformation of the (2+1)-dimensional cmKdV equation* (3) *is*

$$\begin{aligned} T_n &= T_n(\lambda; \lambda_1, \lambda_2, \ldots, \lambda_n) \\ &= \frac{1}{W_{2n}} \begin{bmatrix} (\widetilde{T_n})_{11} & (\widetilde{T_n})_{12} \\ (\widetilde{T_n})_{21} & (\widetilde{T_n})_{22} \end{bmatrix}, \end{aligned} \quad (7)$$

where we have as in (8)–(12).

Comparing (5) and (7), we get

$$(D_{n-1})_{11} = \frac{\widetilde{(D_{n-1})_{11}}}{W_{2n}}, \quad (13)$$

$$(D_{n-1})_{12} = \frac{\widetilde{(D_{n-1})_{12}}}{W_{2n}}, \quad (14)$$

$$(D_{n-1})_{21} = \frac{\widetilde{(D_{n-1})_{21}}}{W_{2n}}, \quad (15)$$

$$(D_{n-2})_{11} = \frac{\widetilde{(D_{n-2})_{11}}}{W_{2n}}, \quad (16)$$

where the numerators are given by (17)–(20). Next, we consider the transformed new solutions $(q^{[n]}, w^{[n]}, v^{[n]})$ of the (2+1)-dimensional cmKdV equation. Under the covariant requirement of the spectral problem, (4) becomes

$$\begin{aligned} \Psi_x^{[n]} &= A^{[n]}\Psi^{[n]} = (\lambda J + A_0^{[n]})\Psi^{[n]}, \\ \Psi_t^{[n]} &= 4\lambda^2\Psi_y^{[n]} + B^{[n]}\Psi^{[n]} \\ &= 4\lambda^2\Psi_y^{[n]} + (\lambda B_1^{[n]} + B_0^{[n]})\Psi^{[n]}. \end{aligned} \quad (21)$$

Then we get

$$\begin{aligned} (T_n)_x &= A^{[n]}T_n - T_n A, \\ (T_n)_t &= 4\lambda^2(T_n)_y + B^{[n]}T_n - T_n B. \end{aligned} \quad (22)$$

Substituting T_n given by Eqn. (5) into Eqns. (22) and taking account of (13)–(16), we get the new n-fold solutions as follows:

$$\begin{aligned} q^{[n]} &= q + 2i\frac{\widetilde{(D_{n-1})_{12}}}{W_{2n}}, \\ w^{[n]} &= w + 4i\left(\frac{\widetilde{(D_{n-1})_{11}}}{W_{2n}}\right)_y, \\ v^{[n]} &= v - 4\left(\frac{\widetilde{(D_{n-1})_{12}}}{W_{2n}}q_y^* - \frac{\widetilde{(D_{n-1})_{21}}}{W_{2n}}q_y\right) \\ &\quad - 8i\left\{\frac{\widetilde{(D_{n-1})_{11}}}{W_{2n}}\left(\frac{\widetilde{(D_{n-1})_{11}}}{W_{2n}}\right)_y \right. \\ &\quad \left. + \left(\frac{\widetilde{(D_{n-1})_{12}}}{W_{2n}}\right)_y \frac{\widetilde{(D_{n-1})_{21}}}{W_{2n}}\right\} \\ &\quad + 8i\left(\frac{\widetilde{(D_{n-2})_{11}}}{W_{2n}}\right)_y. \end{aligned} \quad (23)$$

After choosing the seed solutions $q = w = v = 0$, (4) becomes

$$\Psi_x = \lambda J\Psi, \quad \Psi_t = 4\lambda^2\Psi_y. \quad (24)$$

Then we obtain the basic eigenfunction

$$\Psi = \begin{bmatrix} e^{-i\lambda x + f(y+4\lambda^2 t))} \\ e^{i\lambda x - f(y+4\lambda^2 t))} \end{bmatrix}, \quad (25)$$

where $f(y + 4\lambda^2 t)$ is a smooth arbitrary function.

$$W_{2n}=\begin{vmatrix} \psi_{11} & \psi_{12} & \lambda_1\psi_{11} & \lambda_1\psi_{12} & \dots & \lambda_1^{n-1}\psi_{11} & \lambda_1^{n-1}\psi_{12} \\ \psi_{21} & \psi_{22} & \lambda_2\psi_{21} & \lambda_2\psi_{22} & \dots & \lambda_2^{n-1}\psi_{21} & \lambda_2^{n-1}\psi_{22} \\ \vdots & \vdots & \vdots & \vdots & \ddots & \vdots & \vdots \\ \psi_{2n,1} & \psi_{2n,2} & \lambda_{2n}\psi_{2n,1} & \lambda_{2n}\psi_{2n,2} & \dots & \lambda_{2n}^{n-1}\psi_{2n,1} & \lambda_{2n}^{n-1}\psi_{2n,2} \end{vmatrix}, \tag{8}$$

$$(\widetilde{T_n})_{11}=\begin{vmatrix} 1 & 0 & \lambda & 0 & \dots & \lambda^{n-1} & 0 & \lambda^n \\ \psi_{11} & \psi_{12} & \lambda_1\psi_{11} & \lambda_1\psi_{12} & \dots & \lambda_1^{n-1}\psi_{11} & \lambda_1^{n-1}\psi_{12} & \lambda_1^n\psi_{11} \\ \psi_{21} & \psi_{22} & \lambda_2\psi_{21} & \lambda_2\psi_{22} & \dots & \lambda_2^{n-1}\psi_{21} & \lambda_2^{n-1}\psi_{22} & \lambda_2^n\psi_{21} \\ \vdots & \vdots & \vdots & \vdots & \ddots & \vdots & \vdots & \vdots \\ \psi_{2n,1} & \psi_{2n,2} & \lambda_{2n}\psi_{2n,1} & \lambda_{2n}\psi_{2n,2} & \dots & \lambda_{2n}^{n-1}\psi_{2n,1} & \lambda_{2n}^{n-1}\psi_{2n,2} & \lambda_{2n}^n\psi_{2n,1} \end{vmatrix}, \tag{9}$$

$$(\widetilde{T_n})_{12}=\begin{vmatrix} 0 & 1 & 0 & \lambda & \dots & 0 & \lambda^{n-1} & 0 \\ \psi_{11} & \psi_{12} & \lambda_1\psi_{11} & \lambda_1\psi_{12} & \dots & \lambda_1^{n-1}\psi_{11} & \lambda_1^{n-1}\psi_{12} & \lambda_1^n\psi_{11} \\ \psi_{21} & \psi_{22} & \lambda_2\psi_{21} & \lambda_2\psi_{22} & \dots & \lambda_2^{n-1}\psi_{21} & \lambda_2^{n-1}\psi_{22} & \lambda_2^n\psi_{21} \\ \vdots & \vdots & \vdots & \vdots & \ddots & \vdots & \vdots & \vdots \\ \psi_{2n,1} & \psi_{2n,2} & \lambda_{2n}\psi_{2n,1} & \lambda_{2n}\psi_{2n,2} & \dots & \lambda_{2n}^{n-1}\psi_{2n,1} & \lambda_{2n}^{n-1}\psi_{2n,2} & \lambda_{2n}^n\psi_{2n,1} \end{vmatrix}, \tag{10}$$

$$(\widetilde{T_n})_{21}=\begin{vmatrix} 1 & 0 & \lambda & 0 & \dots & \lambda^{n-1} & 0 & 0 \\ \psi_{11} & \psi_{12} & \lambda_1\psi_{11} & \lambda_1\psi_{12} & \dots & \lambda_1^{n-1}\psi_{11} & \lambda_1^{n-1}\psi_{12} & \lambda_1^n\psi_{12} \\ \psi_{21} & \psi_{22} & \lambda_2\psi_{21} & \lambda_2\psi_{22} & \dots & \lambda_2^{n-1}\psi_{21} & \lambda_2^{n-1}\psi_{22} & \lambda_2^n\psi_{22} \\ \vdots & \vdots & \vdots & \vdots & \ddots & \vdots & \vdots & \vdots \\ \psi_{2n,1} & \psi_{2n,2} & \lambda_{2n}\psi_{2n,1} & \lambda_{2n}\psi_{2n,2} & \dots & \lambda_{2n}^{n-1}\psi_{2n,1} & \lambda_{2n}^{n-1}\psi_{2n,2} & \lambda_{2n}^n\psi_{2n,2} \end{vmatrix}, \tag{11}$$

$$(\widetilde{T_n})_{22}=\begin{vmatrix} 0 & 1 & 0 & \lambda & \dots & 0 & \lambda^{n-1} & \lambda^n \\ \psi_{11} & \psi_{12} & \lambda_1\psi_{11} & \lambda_1\psi_{12} & \dots & \lambda_1^{n-1}\psi_{11} & \lambda_1^{n-1}\psi_{12} & \lambda_1^n\psi_{12} \\ \psi_{21} & \psi_{22} & \lambda_2\psi_{21} & \lambda_2\psi_{22} & \dots & \lambda_2^{n-1}\psi_{21} & \lambda_2^{n-1}\psi_{22} & \lambda_2^n\psi_{22} \\ \vdots & \vdots & \vdots & \vdots & \ddots & \vdots & \vdots & \vdots \\ \psi_{2n,1} & \psi_{2n,2} & \lambda_{2n}\psi_{2n,1} & \lambda_{2n}\psi_{2n,2} & \dots & \lambda_{2n}^{n-1}\psi_{2n,1} & \lambda_{2n}^{n-1}\psi_{2n,2} & \lambda_{2n}^n\psi_{2n,2} \end{vmatrix}. \tag{12}$$

The order-n deformed solitons can be obtained by (23) with the following eigenfunction:

$$\begin{aligned} \psi_{2k-1,1} &= \exp(-i\lambda_{2k-1}x + f_{2k-1}), \\ \psi_{2k-1,2} &= \exp(i\lambda_{2k-1}x - f_{2k-1}), \\ \psi_{2k,1} &= -\exp(-i\lambda_{2k}x + f_{2k}), \\ \psi_{2k,2} &= \exp(i\lambda_{2k}x - f_{2k}), \end{aligned} \tag{26}$$

where $\lambda_{2k}=\lambda_{2k-1}^*, f_{2k}=f_{2k-1}^*=f(y+4\lambda_{2k-1}^2t), k=1,\dots,n$.

3. Order-1 deformed soliton solutions

In this section, we focus on the order-1 deformed solitons of (3). Setting $k=1$ in (26), we get

$$\begin{aligned} \psi_{11} &= \exp(-i\lambda_1x + f_1 + \delta_1), \\ \psi_{12} &= \exp(i\lambda_1x - f_1 - \delta_1), \\ \psi_{21} &= -\exp(-i\lambda_2x - f_2 - \delta_1), \\ \psi_{22} &= \exp(i\lambda_2x + f_2 + \delta_1). \end{aligned} \tag{27}$$

Then we choose three typical illustrative examples. Since we have

$$w^{[1]} = 2\int (|q^{[1]}|^2)_y \,\mathrm{d}x,$$

$$v^{[1]} = -2i\int (q_{xy}^{[1]}q^{[1]*} - q^{[1]}q_{xy}^{[1]*})\,\mathrm{d}x,$$

we just analyze $|q^{[1]}|$ minutely in this section.

3.1. Polynomial type. If we choose $f_1=\mu_1(y+4\lambda_1^2t)^m$, $f_2=\mu_2(y+4\lambda_2^2t)^m$, the solutions given by (23) and (27) are defined by (28) , where μ_1,μ_2 are complex constants satisfying $\mu_1=\mu_2^*$, δ_1 is a real constant and m is a positive integer greater than 1. It is worth noting that, if $m<0$, the eigenfunction is singular at $t=0$, $y=0$; if $m=1$, the solution is a soliton given by Yesmakhanova *et al*. (2017). For convenience, we write

$$\mathcal{A}=y+(4\alpha_1^2-4\beta_1^2)t, \quad \mathcal{B}=8\alpha_1\beta_1t, \tag{29}$$

and

$$\begin{aligned} &\lambda_1=\alpha_1+\beta_1 i, \quad \lambda_2=\alpha_1-\beta_1 i, \\ &\mu_1=\eta_1+\xi_1 i, \quad \mu_2=\eta_1-\xi_1 i. \end{aligned} \tag{30}$$

$$(\widetilde{D_{n-1}})_{11}=\begin{vmatrix} \psi_{11} & \psi_{12} & \lambda_1\psi_{11} & \lambda_1\psi_{12} & \dots & \lambda_1^{n-2}\psi_{12} & \lambda_1^{n-1}\psi_{12} & \lambda_1^{n}\psi_{11} \\ \psi_{21} & \psi_{22} & \lambda_2\psi_{21} & \lambda_2\psi_{22} & \dots & \lambda_2^{n-2}\psi_{22} & \lambda_2^{n-1}\psi_{22} & \lambda_2^{n}\psi_{21} \\ \vdots & \vdots & \vdots & \vdots & \ddots & \vdots & \vdots & \vdots \\ \psi_{2n,1} & \psi_{2n,2} & \lambda_{2n}\psi_{2n,1} & \lambda_{2n}\psi_{2n,2} & \dots & \lambda_{2n}^{n-2}\psi_{2n,2} & \lambda_{2n}^{n-1}\psi_{2n,2} & \lambda_{2n}^{n}\psi_{2n,1} \end{vmatrix}, \tag{17}$$

$$(\widetilde{D_{n-1}})_{12}=-\begin{vmatrix} \psi_{11} & \psi_{12} & \lambda_1\psi_{11} & \lambda_1\psi_{12} & \dots & \lambda_1^{n-2}\psi_{12} & \lambda_1^{n-1}\psi_{11} & \lambda_1^{n}\psi_{11} \\ \psi_{21} & \psi_{22} & \lambda_2\psi_{21} & \lambda_2\psi_{22} & \dots & \lambda_1^{n-2}\psi_{22} & \lambda_2^{n-1}\psi_{21} & \lambda_2^{n}\psi_{21} \\ \vdots & \vdots & \vdots & \vdots & \ddots & \vdots & \vdots & \vdots \\ \psi_{2n,1} & \psi_{2n,2} & \lambda_{2n}\psi_{2n,1} & \lambda_{2n}\psi_{2n,2} & \dots & \lambda_1^{n-2}\psi_{2n,2} & \lambda_{2n}^{n-1}\psi_{2n,1} & \lambda_{2n}^{n}\psi_{2n,1} \end{vmatrix}, \tag{18}$$

$$(\widetilde{D_{n-1}})_{21}=\begin{vmatrix} \psi_{11} & \psi_{12} & \lambda_1\psi_{11} & \lambda_1\psi_{12} & \dots & \lambda_1^{n-2}\psi_{12} & \lambda_1^{n-1}\psi_{12} & \lambda_1^{n}\psi_{12} \\ \psi_{21} & \psi_{22} & \lambda_2\psi_{21} & \lambda_2\psi_{22} & \dots & \lambda_2^{n-2}\psi_{22} & \lambda_2^{n-1}\psi_{22} & \lambda_2^{n}\psi_{22} \\ \vdots & \vdots & \vdots & \vdots & \ddots & \vdots & \vdots & \vdots \\ \psi_{2n,1} & \psi_{2n,2} & \lambda_{2n}\psi_{2n,1} & \lambda_{2n}\psi_{2n,2} & \dots & \lambda_{2n}^{n-2}\psi_{2n,2} & \lambda_{2n}^{n-1}\psi_{2n,2} & \lambda_{2n}^{n}\psi_{2n,2} \end{vmatrix}, \tag{19}$$

$$(\widetilde{D_{n-2}})_{11}=\begin{vmatrix} \psi_{11} & \psi_{12} & \lambda_1\psi_{11} & \lambda_1\psi_{12} & \dots & \lambda_1^{n-3}\psi_{12} & \lambda_1^{n-2}\psi_{12} & \lambda_1^{n-1}\psi_{11} & \lambda_1^{n-1}\psi_{12} & \lambda_1^{n}\psi_{11} \\ \psi_{21} & \psi_{22} & \lambda_2\psi_{21} & \lambda_2\psi_{22} & \dots & \lambda_2^{n-3}\psi_{22} & \lambda_2^{n-2}\psi_{22} & \lambda_2^{n-1}\psi_{21} & \lambda_2^{n-1}\psi_{22} & \lambda_2^{n}\psi_{21} \\ \vdots & \vdots & \vdots & \vdots & \ddots & \vdots & \vdots & \vdots & \vdots & \vdots \\ \psi_{2n,1} & \psi_{2n,2} & \lambda_{2n}\psi_{2n,1} & \lambda_{2n}\psi_{2n,2} & \dots & \lambda_{2n}^{n-3}\psi_{2n,2} & \lambda_{2n}^{n-2}\psi_{2n,2} & \lambda_{2n}^{n-1}\psi_{2n,1} & \lambda_{2n}^{n-1}\psi_{2n,2} & \lambda_{2n}^{n}\psi_{2n,1} \end{vmatrix}. \tag{20}$$

$$\begin{aligned} q^{[1]} &= -\frac{i(\lambda_1-\lambda_2)\exp(-i(\lambda_1+\lambda_2)x+\mu_1(y+4\lambda_1^2t)^m-\mu_2(y+4\lambda_2^2t)^m)}{\cosh(-i(\lambda_1-\lambda_2)x+\mu_1(y+4\lambda_1^2t)^m+\mu_2(y+4\lambda_2^2t)^m+2\delta_1)}, \\ w^{[1]} &= -\frac{2mi(\lambda_1-\lambda_2)(\mu_1(y+4\lambda_1^2t)^{m-1}+\mu_2(y+4\lambda_2^2t)^{m-1})}{\cosh^2(-i(\lambda_1-\lambda_2)x+\mu_1(y+4\lambda_1^2t)^m+\mu_2(y+4\lambda_2^2t)^m+2\delta_1)}, \\ v^{[1]} &= \frac{4mi(\lambda_1-\lambda_2)(\lambda_1\mu_1(y+4\lambda_1^2t)^{m-1}+\lambda_2\mu_2(y+4\lambda_2^2t)^{m-1})}{\cosh^2(-i(\lambda_1-\lambda_2)x+\mu_1(y+4\lambda_1^2t)^m+\mu_2(y+4\lambda_2^2t)^m+2\delta_1)}. \end{aligned} \tag{28}$$

Here α_1, β_1, η_1, ξ_1 are real constants. Then $|q^{[1]}|$ is in the form of (31).

By solving the equation $|q^{[1]}|_x=0$, we can obtain the trajectory of $|q^{[1]}|$ as follows:

$$\begin{aligned} x=&-\frac{\delta_1}{\beta_1}-\frac{1}{2\beta_1}((\eta_1+i\xi_1)(\mathcal{A}+\mathcal{B}i)^m \\ &+(\eta_1-i\xi_1)(\mathcal{A}-\mathcal{B}i)^m). \end{aligned} \tag{32}$$

The expressions (31) and (32) are real functions and (32) is a polynomial function. Therefore, we call this deformed soliton solution a polynomial type soliton solution. We can obtain denumerable kinds of deformed solitons theoretically. Substituting (32) into (31), we obtain that the amplitude is $2\beta_1$ and is independent of m. Next, we give two specific cases for analysis.

Case $m=2$. We have the expression (33), and the trajectory is

$$\begin{aligned} x=&-\frac{\delta_1}{\beta_1}-\frac{1}{\beta_1}(\eta_1y^2+(8\alpha_1^2\eta_1-16\alpha_1\beta_1\xi_1 \\ &-8\beta_1^2\eta_1)yt+(16\eta_1(\alpha_1^4-6\alpha_1^2\beta_1^2+\beta_1^4) \\ &-64\xi_1\alpha_1\beta_1(\alpha_1^2-\beta_1^2))t^2). \end{aligned} \tag{34}$$

Then we find out that the trajectory is a parabola at any moment and its shape changes over time. Therefore, we name this soliton a parabolic one. Figure 1 shows the 3D map, density figure, and trajectories. The velocity in the $(x,\ y)$-direction is $(128\alpha_1^2\beta_1\eta_1t,\ -4(\alpha_1^2-\beta_1^2))$. It is easy to check that $|q^{[1]}(x,y,t)|=|q^{[1]}(x,-y,-t)|$. This means that the parabolic soliton has the same shape at times t and $-t$, but the position is symmetric with respect to the plane $x=0$. The symmetry is shown in Fig. 1(c).

Case $m=3$. We have that $|q^{[1]}|$ is given by (35). The trajectory of $|q^{[1]}|$ is

$$x=-\frac{\delta_1}{\beta_1}-\frac{1}{\beta_1}(\eta_1y^3+(12\alpha_1^2\eta_1-24\alpha_1\beta_1\xi_1$$

$$|q^{[1]}| = \frac{2\beta_1}{\cosh(2\beta_1 x + (\eta_1 + i\xi_1)(\mathcal{A} + \mathcal{B}i)^m + (\eta_1 - i\xi_1)(\mathcal{A} - \mathcal{B}i)^m + 2\delta_1)}. \tag{31}$$

$$|q^{[1]}| = \frac{2\beta_1}{\cosh(2\beta_1 x + 2\eta_1(\mathcal{A}^2 - \mathcal{B}^2) - 4\xi_1\mathcal{A}\mathcal{B} + 2\delta_1)}. \tag{33}$$

$$|q^{[1]}| = \frac{2\beta_1}{\cosh(2\beta_1 x + 2\eta_1\mathcal{A}^3 + 2\xi_1\mathcal{B}^3 - 6\eta_1\mathcal{A}\mathcal{B}^2 - 6\xi_1\mathcal{A}^2\mathcal{B} + 2\delta_1)}. \tag{35}$$

$$\begin{aligned} &- 12\beta_1^2\eta_1)y^2t + (48\eta_1(\alpha_1^4 - 6\alpha_1^2\beta_1^2 + \beta_1^4) \\ &- 192\alpha_1\beta_1\xi_1(\alpha_1^2 - \beta_1^2))yt^2 + (64\eta_1(\alpha_1^6 \\ &- 15\alpha_1^4\beta_1^2 + 15\alpha_1^2\beta_1^4 - \beta_1^6) - 128\xi_1(3\alpha_1^5\beta_1 \\ &- 10\alpha_1^3\beta_1^3 + 3\alpha_1\beta_1^5))t^3). \end{aligned} \tag{36}$$

Then we find out that the trajectory is a cubic function over time. That is why we name this kind of deformed soliton a cubic one. Figure 2 shows the 3D map, density figure, and trajectories. The velocity in $(x,\ y)$-direction is $(-1536\alpha_1^3\beta_1^2\xi_1 t^2,\ -4(\alpha_1^2 - \beta_1^2))$. It is easy to check that $|q^{[1]}(x, y, t)| = |q^{[1]}(-x - 2\delta_1/\beta_1, -y, -t)|$. This means the parabolic soliton has the same shape on the time t and $-t$, but the position is symmetric with respect to $x = -\delta_1/\beta_1,\ y = 0$. The symmetry is shown in Fig. 2(c). If we choose

$$f_1 = \mu_1 \sum_{j=2}^{N} c_j(y + 4\lambda_1^2 t)^j),$$

$$f_2 = \mu_2 \sum_{j=2}^{N} c_j(y + 4\lambda_2^2 t)^j)$$

(N is a positive integer), we can obtain the eigenfunctions as follows:

$$\begin{aligned} \psi_{11} &= \exp(-i\lambda_1 x + \mu_1 \sum_{j=2}^{N} c_j(y + 4\lambda_1^2 t)^j + \delta_1), \\ \psi_{12} &= \exp(i\lambda_1 x - \mu_1 \sum_{j=2}^{N} c_j(y + 4\lambda_1^2 t)^j + \delta_1), \\ \psi_{21} &= -\exp(-i\lambda_2 x - \mu_2 \sum_{j=2}^{N} c_j(y + 4\lambda_2^2 t)^j + \delta_1), \\ \psi_{22} &= \exp(i\lambda_2 x + \mu_2 \sum_{j=2}^{N} c_j(y + 4\lambda_2^2 t)^j + \delta_1), \end{aligned} \tag{37}$$

where c_j are integers and at least one of them is nonzero. Substituting (37) into (23), we can rewrite $q^{[1]}$ as (38), from which (39) follows. Solving the equation$|q^[1]|_\lambda x = 0$, we get (40). After simplification, we get the trajectory (41).

3.2. Trigonometric type. If we choose $f_1 = \mu_1 \sin^m(y + 4\lambda_1^2 t)$, $f_2 = \mu_2 \sin^m(y + 4\lambda_2^2 t)$, the expressions of the solutions given by (23) and (27) are given by (42), where $\mu_1 = \mu_2^*$, δ_1 is a real constant and m is a positive integer. We called this kind of solution a trigonometric one. It is obvious that $q^{[1]}(x, y, t) = q^{[1]}(x, y + 2\pi, t)$. So $q^{[1]}$ of (42) has a period 2π in the y-direction. Solving $|q^{[1]}|_x = 0$, we can obtain the trajectory

$$\begin{aligned} x = -\frac{1}{\lambda_1 - \lambda_2}\Big[&i(\mu_1 \sin^m(y + 4\lambda_1^2 t) \\ &+ \mu_2 \sin^m(y + 4\lambda_2^2 t) + 2\delta_1)\Big]. \end{aligned} \tag{43}$$

Substituting (43) into $|q^{[1]}|$, we get the amplitude $2\beta_1$. Then we analyze two examples in detail. Without loss of generality, we assume $\beta_1 > 0$.

Case $m = 1$. We have

$$\begin{aligned} |q^{[1]}| =& 2\beta_1/\cosh(2\beta_1 x + 2\eta_1 \sin\mathcal{A}\cosh\mathcal{B} \\ &- 2\xi_1 \cos\mathcal{A}\sinh\mathcal{B} + 2\delta_1), \end{aligned} \tag{44}$$

and the trajectory is

$$x = -\frac{\eta_1 \sin\mathcal{A}\cosh\mathcal{B} - \xi_1 \cos\mathcal{A}\sinh\mathcal{B} + \delta_1}{\beta_1}. \tag{45}$$

Figure 3 shows the 3D map and trajectories. It is interesting to see that the trajectory (45) is a carrier wave on the $(x,\ y)$-plane and its amplitude is minimum at $t = 0$, which grows with the increase in $|t|$. The velocity of $|q^{[1]}(x, y, t)|$ in the $(x,\ y)$-direction is $(8\alpha_1\xi_1\cosh(8\alpha_1\beta_1 t),\ -4(\alpha_1^2 - \beta_1^2))$. It is easy to see that $|q^{[1]}(x, y, t)| = |q^{[1]}(-x - 2\delta_1/\beta_1, -y, -t)|$. This means the soliton has the same shape on the time t and $-t$, but the position is symmetric with respect to $x = -\delta_1/\beta_1,\ y = 0$. The symmetries are also shown in Fig. 3(c).

Case $m = 3$. We have

$$|q^{[1]}| = \frac{2\beta_1}{\cosh(2\beta_1 x + 2\eta_1 C - 2\xi_1 D + 2\delta_1)}, \tag{46}$$

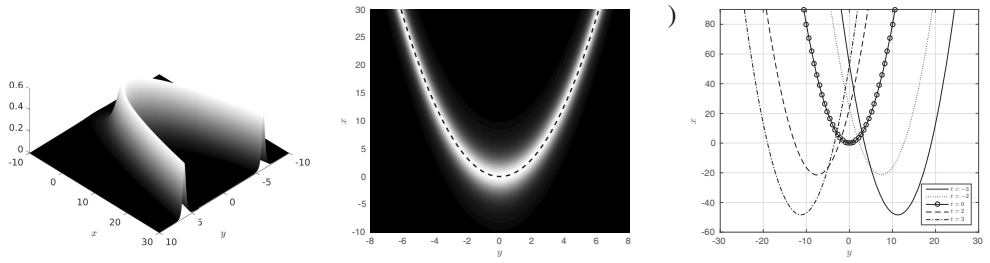

(a) (b) (c)

Fig. 1. $|q^{[1]}|$ (33) with $\delta_1 = 0$, $\alpha_1 = 2/3$, $\beta_1 = 1/4$, $\eta_1 = -1/5$, $\xi_1 = 1/3$: 3D figure at $t = 0$ (a), density figure at $t = 0$ and the dashed curve in the center represents trajectories (34) (b); the trajectories (34) (c).

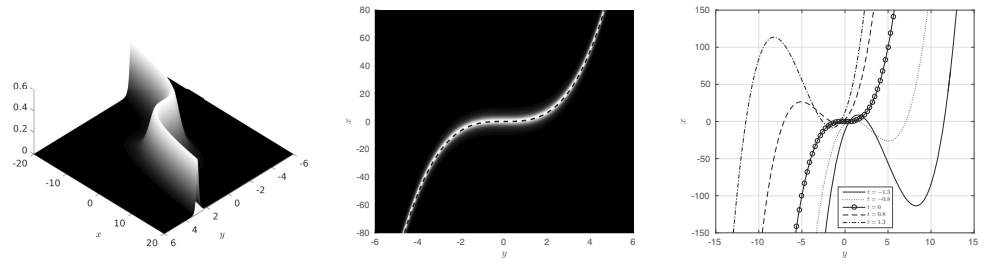

(a) (b) (c)

Fig. 2. $|q^{[1]}|$ (35) with $\delta_1 = 0$, $\alpha_1 = 2/3$, $\beta_1 = 1/4$, $\eta_1 = -1/5$, $\xi_1 = 1/3$: 3D figure at $t = 0$ (a), density figure at $t = 0$ and the dashed curve in the center represents the trajectories (36) (b), trajectories (36) (c).

and the trajectory is

$$x = -\frac{\eta_1 C - \xi_1 D + \delta_1}{\beta_1}. \tag{47}$$

Here

$$C = \sin^3 \mathcal{A} \cosh^3 \mathcal{B} - 3 \sin \mathcal{A} \cos^2 \mathcal{A} \sinh^2 \mathcal{B} \cosh \mathcal{B},$$
$$D = \sinh^3 \mathcal{A} \cos^3 \mathcal{B} - 3 \sin^2 \mathcal{A} \cos \mathcal{A} \sinh \mathcal{B} \cosh^2 \mathcal{B}.$$

Figure 4 shows the 3D map and trajectories. It is different from (45), which is a carrier wave. The trajectory (47) is a periodic modulating wave on the (x, y)-plane, and each period in the x-direction has three different peaks. The velocity in the (x, y)-direction is $(-24\alpha_1\xi_1 \cosh(8\alpha_1\beta_1 t) \sinh^2(8\alpha_1\beta_1 t), -4(\alpha_1^2 - \beta_1^2))$. It is easy to check that $|q^{[1]}(x, y, t)| = |q^{[1]}(-x - 2\delta_1/\beta_1, -y, -t)|$. This means that the soliton has the same shape at t and $-t$, but the position is symmetric with respect to $x = -\delta_1/\beta_1$, $y = 0$. The symmetries are also shown in Fig. 4(c).

3.3. Hyperbolic type. If we choose $f_1 = \mu_1 \sinh^m(y + 4\lambda_1^2 t)$, $f_2 = \mu_2 \sinh^m(y + 4\lambda_2^2 t)$, the expressions of the solution given by (23) and (27) are given by (48), where $\mu_1 = \mu_2^*$, δ_1 is a real constant and m is a positive integer. We called this kind of solution a hyperbolic one. Through solving $|q^{[1]}|_x = 0$, we can obtain the trajectory

$$x = -i(\mu_1 \sinh^m(y + 4\lambda_1^2 t) + \mu_2 \sinh^m(y + 4\lambda_2^2 t) + 2\delta_1)/\lambda_1 - \lambda_2 \tag{49}$$

Substituting (43) into $|q^{[1]}|$, we get the amplitude $2\beta_1$. Then we analyze two examples in detail.

Case $m = 1$. We have

$$|q^{[1]}| = 2\beta_1 / \cosh(2\beta_1 x + 2\eta_1 \sinh \mathcal{A} \cos \mathcal{B} - 2\xi_1 \cosh \mathcal{A} \sin \mathcal{B} + 2\delta_1), \tag{50}$$

and the trajectory is

$$x = -\frac{\eta_1 \sinh \mathcal{A} \cos \mathcal{B} - \xi_1 \cosh \mathcal{A} \sin \mathcal{B} + \delta_1}{\beta_1}. \tag{51}$$

Figure 5 shows the 3D map and trajectories at different times. The velocity in the (x, y)-direction is $(8\alpha_1\xi_1 \cos(8\alpha_1\beta_1 t), -4(\alpha_1^2 - \beta_1^2))$. It is easy to get $|q^{[1]}(x, y, t)| = |q^{[1]}(-x - 2\delta_1/\beta_1, -y, -t)|$. This means that the soliton has the same shape at times t and $-t$, but the position is symmetric with respect to $x = -\delta_1/\beta_1$, $y = 0$. The symmetry is shown in Fig. 5(c).

Case $m = 2$. We have (52) and the trajectory is given by (53).

$$q^{[1]}=\frac{i(\lambda_1-\lambda_2)\exp(-i(\lambda_1+\lambda_2)x+\mu_1\sum\limits_{j=2}^{N}c_j(y+4\lambda_1^2t)^j-\mu_2\sum\limits_{j=2}^{N}c_j(y+4\lambda_2^2t)^j)}{\cosh(i(\lambda_1-\lambda_2)x-\mu_1\sum\limits_{j=2}^{N}c_j(y+4\lambda_1^2t)^j-\mu_2\sum\limits_{j=2}^{N}c_j(y+4\lambda_2^2t)^j)}. \tag{38}$$

$$|q^{[1]}|=\frac{2\beta_1}{\cosh(2\beta_1x+(\eta_1+\xi_1i)\sum\limits_{j=2}^{N}c_j(\mathcal{A}+\mathcal{B}i)^j+(\eta_1-\xi_1i)\sum\limits_{j=2}^{N}c_j(\mathcal{A}-\mathcal{B}i)^j)+2\delta_1}. \tag{39}$$

$$x=-\frac{(\eta_1+\xi_1i)\sum\limits_{j=2}^{N}c_j(\mathcal{A}+\mathcal{B}i)^j+(\eta_1-\xi_1i)\sum\limits_{j=2}^{N}c_j(\mathcal{A}-\mathcal{B}i)^j}{2\beta}-\frac{\delta_1}{\beta_1}. \tag{40}$$

$$x=-\frac{\eta_1\sum\limits_{j=2}^{N}\left(c_j\sum\limits_{k=0}^{[\frac{j}{2}]}(-1)^k\mathbb{C}_j^{2k}\mathcal{A}^{2k}\mathcal{B}^{j-2k}\right)-\xi_1\sum\limits_{j=2}^{N}\left(c_j\sum\limits_{k=0}^{[\frac{j}{2}]}\mathbb{C}_j^{2k+1}\mathcal{A}^{2k+1}\mathcal{B}^{j-2k-1}\right)}{\beta}-\frac{\delta_1}{\beta_1}. \tag{41}$$

$$\begin{aligned}
q^{[1]}&=-\frac{i(\lambda_1-\lambda_2)\exp(-i(\lambda_1+\lambda_2)x+\mu_1\sin^m(y+4\lambda_1^2t)-\mu_2\sin^m(y+4\lambda_2^2t))}{\cosh(-i(\lambda_1-\lambda_2)x+\mu_1\sin^m(y+4\lambda_1^2t)+\mu_2\sin^m(y+4\lambda_2^2t)+2\delta_1)},\\
w^{[1]}&=2mi\frac{(\lambda_1-\lambda_2)(\mu_1\sin^{m-1}(y+4\lambda_1^2t)\cos(y+4\lambda_2^2t)+\mu_2\sin^{m-1}(y+4\lambda_2^2t)\cos(y+4\lambda_2^2t))}{\cosh^2(-i(\lambda_1-\lambda_2)x+\mu_1\sin^m(y+4\lambda_1^2t)+\mu_2\sin^m(y+4\lambda_2^2t)+2\delta_1)},\\
v^{[1]}&=4mi\frac{(\lambda_1-\lambda_2)(\lambda_1\mu_1\sinh^{m-1}(y+4\lambda_1^2t)\cos(y+4\lambda_1^2t)+\lambda_2\mu_2\sinh^{m-1}(y+4\lambda_2^2t)\cos(y+4\lambda_2^2t))}{\cosh^2(-i(\lambda_1-\lambda_2)x+\mu_1\sin^m(y+4\lambda_1^2t)+\mu_2\sin^m(y+4\lambda_2^2t)+2\delta_1)}.
\end{aligned} \tag{42}$$

$$\begin{aligned}
q^{[1]}&=-\frac{i(\lambda_1-\lambda_2)\exp(-i(\lambda_1+\lambda_2)x+\mu_1\sinh^m(y+4\lambda_1^2t)-\mu_2\sinh^m(y+4\lambda_2^2t))}{\cosh(-i(\lambda_1-\lambda_2)x+\mu_1\sinh^m(y+4\lambda_1^2t)+\mu_2\sinh^m(y+4\lambda_2^2t)+2\delta_1)},\\
w^{[1]}&=-2mi\frac{(\lambda_1-\lambda_2)(\mu_1\sinh^{m-1}(y+4\lambda_1^2t)\cosh(y+4\lambda_2^2t)+\mu_2\sinh^{m-1}(y+4\lambda_2^2t)\cosh(y+4\lambda_2^2t))}{\cosh^2(-i(\lambda_1-\lambda_2)x+\mu_1\sinh^m(y+4\lambda_1^2t)+\mu_2\sinh^m(y+4\lambda_2^2t)+2\delta_1)},\\
v^{[1]}&=4mi\frac{(\lambda_1-\lambda_2)^2(\lambda_1\mu_1\sinh^{m-1}(y+4\lambda_1^2t)\cosh(y+4\lambda_1^2t)+\lambda_2\mu_2\sinh^{m-1}(y+4\lambda_2^2t)\cosh(y+4\lambda_2^2t))}{\cosh^2(-i(\lambda_1-\lambda_2)x+\mu_1\sinh^m(y+4\lambda_1^2t)+\mu_2\sinh^m(y+4\lambda_2^2t)+2\delta_1)}.
\end{aligned} \tag{48}$$

$$|q^{[1]}|=\frac{2\beta_1}{\cosh(2\beta_1x+2\eta_1(\sinh^2\mathcal{A}\cos^2\mathcal{B}-\cosh^2\mathcal{A}\sin^2\mathcal{B})-4\xi_1\sinh\mathcal{A}\cosh\mathcal{A}\sin\mathcal{B}\cos\mathcal{B}+2\delta_1)}, \tag{52}$$

$$x=-\frac{\eta_1(\sinh^2\mathcal{A}\cos^2\mathcal{B}-\cosh^2\mathcal{A}\sin^2\mathcal{B})-2\xi_1\sinh\mathcal{A}\cosh\mathcal{A}\sin\mathcal{B}\cos\mathcal{B}+\delta_1}{\beta_1}. \tag{53}$$

Figure 6 shows the 3D map and trajectories at different times. The velocity in the (x, y)-direction is $(8\alpha_1\xi_1 \sin(16\alpha_1\beta_1 t), -4(\alpha_1^2 - \beta_1^2))$. It is easy to check that $|q^{[1]}(x, y, t)| = |q^{[1]}(-x - 2\delta_1/\beta_1, -y, -t)|$. This means the soliton has the same shape at time t and $-t$, but the position is symmetric with respect to $x = -\delta_1/\beta_1$, $y = 0$. The symmetry is shown in Fig. 6(c).

We can also take f_1 and f_2 as any other smooth functions, and the calculation method is the same as mentioned above. Hence we do not list them all.

Theorem 2. *If we choose $f_1 = f_1(y + 4\lambda_1^2 t)$, $f_2 = f_1^*$ as smooth functions, the order-1 solution is*

$$\begin{aligned} q^{[1]} &= -\frac{(\lambda_1 - \lambda_2)\exp(-i(\lambda_1 + \lambda_2) + f_1 - f_2)}{\cosh(-i(\lambda_1 - \lambda_2)x + f_1 + f_2 + 2\delta_1)}, \\ w^{[1]} &= -\frac{2i(\lambda_1 - \lambda_2)(f_1^{'} + f_2^{'})}{\cosh^2(-i(\lambda_1 - \lambda_2)x + f_1 + f_2 + 2\delta_1)}, \\ v^{[1]} &= \frac{4i(\lambda_1 - \lambda_2)(\lambda_1 f_1^{'} + \lambda_2 f_2^{'})}{\cosh^2(-i(\lambda_1 - \lambda_2)x + f_1 + f_2 + 2\delta_1)}, \end{aligned} \tag{54}$$

where $f_1^{'} = \partial f_1/\partial y, f_2^{'} = \partial f_2/\partial y$. The trajectory of $|q^{[1]}|$ is

$$x = \frac{f_1 + f_2 + 2\delta_1}{i(\lambda_1 - \lambda_2)}. \tag{55}$$

The periodicity and symmetry of the function are determined by f_k.

4. Order-2 deformed soliton solutions

In this section, we discuss order-2 deformed solitons. If we choose $f_1 = f_1(y + 4\lambda_1^2 t)$, $f_3 = f_3(y + 4\lambda_3^2 t)$ and $f_2 = f_1^*$, $f_4 = f_3^*$, we can obtain the eigenfunction as

$$\begin{aligned} \psi_{11} &= \exp(-i\lambda_1 x + f_1 + \delta_1), \\ \psi_{12} &= \exp(i\lambda_1 x - f_1 - \delta_1), \\ \psi_{21} &= -\exp(-i\lambda_2 x - f_2 - \delta_1), \\ \psi_{22} &= \exp(i\lambda_2 x + f_2 + \delta_1), \\ \psi_{31} &= \exp(-i\lambda_3 x + f_3 + \delta_2), \\ \psi_{32} &= \exp(i\lambda_3 x - f_3 - \delta_2), \\ \psi_{41} &= -\exp(-i\lambda_4 x - f_4 - \delta_2), \\ \psi_{42} &= \exp(i\lambda_4 x + f_4 + \delta_2), \end{aligned} \tag{56}$$

where δ_k is a real constant. Using the same method as in the previous section, we can obtain many kinds of order-2 deformed solitons from (23). Because the formulas of $v^{[2]}$ and $w^{[2]}$ are complicated, we just give a simplified formula of $q^{[2]}$ as (44). Then we have (46).

Figure 7 shows four examples of $|q^{[2]}|$ which involved different cases of f_k: (a) shows an order-2 parabola soliton where $f_k = \mu_k(y + 4\lambda_k^2 t)^2$; (b) shows an order-2 trigonometric type solution where $f_k = \mu_k \sin(y + 4\lambda_k^2 t)$; (c) shows a mixed type solution consisting of a trigonometric type soliton and a normal soliton where $f_1 = \mu_1(y + 4\lambda_1^2 t)$, $f_3 = \mu_3 \sin(y + 4\lambda_3^2 t)$; (d) shows a mixed type consisting of a parabola soliton and a hyperbolic type soliton where $f_1 = \mu_1(y + 4\lambda_1^2 t)^2$, $f_3 = \mu_3 \sinh(y + 4\lambda_3^2 t)$. Let us now choose two examples to show the time evolution.

Case 1: Choosing $f_k = \mu_k(y + 4\lambda_k^2 t)^2$ in (56), we have

$$\begin{aligned} \Lambda_1 &= \beta_1 x + \eta_1 y^2 + (8\eta_1(\alpha_1^2 - \beta_1^2) - 16\alpha_1\beta_1\xi_1)yt \\ &\quad + (16\eta_1(\alpha_1^4 - 6\alpha_1^2\beta_1^2 + \beta_1^4) \\ &\quad - 64\xi_1\alpha_1\beta_1(\alpha_1^2 - \beta_1^2))t^2 + \delta_1, \\ \Lambda_2 &= \beta_2 x + \eta_2 y^2 + (8\eta_2(\alpha_2^2 - \beta_2^2) - 16\alpha_2\beta_2\xi_2)yt \\ &\quad + (16\eta_2(\alpha_2^4 - 6\alpha_2^2\beta_2^2 + \beta_2^4) \\ &\quad - 64\xi_2\alpha_2\beta_2(\alpha_2^2 - \beta_2^2))t^2 + \delta_2, \\ \Gamma_1 &= \alpha_1 x + \xi_1 y^2 + (8\xi_1(\alpha_1^2 - \beta_1^2) + 16\alpha_1\beta_1\eta_1)yt \\ &\quad + (16\xi_1(\alpha_1^4 - 6\alpha_1^2\beta_1^2 + \beta_1^4) \\ &\quad + 64\eta_1\alpha_1\beta_1(\alpha_1^2 - \beta_1^2))t^2 + \delta_1, \\ \Gamma_2 &= \alpha_2 x + \xi_2 y^2 + (8\xi_2(\alpha_2^2 - \beta_2^2) + 16\alpha_2\beta_2\eta_2)yt \\ &\quad + (16\xi_2(\alpha_2^4 - 6\alpha_2^2\beta_2^2 + \beta_2^4) \\ &\quad + 64\eta_2\alpha_2\beta_2(\alpha_2^2 - \beta_2^2))t^2 + \delta_2. \end{aligned} \tag{60}$$

It is obvious that $|q^{[2]}(x, y, t)| = |q^{[2]}(x, -y, -t)|$. This means that the evolution of $|q^{[2]}|$ over time also has the same symmetry with (33). Figure 8 shows the symmetry and evolution over time.

Case 2. Choosing $f_1 = \mu_1(y + 4\lambda_1^2 t)$, $f_3 = \mu_3 \sin(y + 4\lambda_3^2 t)$ in (56), we have

$$\begin{aligned} \Lambda_1 &= \beta_1 x + \eta_1(y + 4(\alpha_1^2 - \beta_1^2)t) - 8\xi_1\alpha_1\beta_1 t + \delta_1, \\ \Gamma_1 &= -\alpha_1 x + \xi_1(y + 4(\alpha_1^2 - \beta_1^2)t) + 8\eta_1\alpha_1\beta_1 t, \\ \Lambda_2 &= \beta_2 x - \xi_2 \cos(y + 4(\alpha_2^2 - \beta_2^2)t)\sinh(8\alpha_2\beta_2 t) \\ &\quad + \eta_2 \sin(y + 4(\alpha_2^2 - \beta_2^2)t)\cosh(8\alpha_2\beta_2 t) + \delta_2, \\ \Gamma_2 &= -\alpha_2 x + \xi_2 \sin(y + 4(\alpha_2^2 - \beta_2^2)t)\cosh(8\alpha_2\beta_2 t) \\ &\quad + \eta_2 \cos(y + 4(\alpha_2^2 - \beta_2^2)t)\sinh(8\alpha_2\beta_2 t). \end{aligned} \tag{61}$$

We can get $|q^{[2]}(x, y, t)| \neq |q^{[2]}(x, -y, -t)|$. This means that the evolution of $|q^{[2]}|$ over time has no symmetry. Figure 9 shows the interaction between a soliton and a trigonometric type soliton.

5. Summary and conclusions

In this paper, we studied the (2+1)-dimensional complex modified Korteweg–de Vries equation. First, we gave the determinant form of the n-fold Darboux transformation. Through the seed solution $q = w = v = 0$ and taking

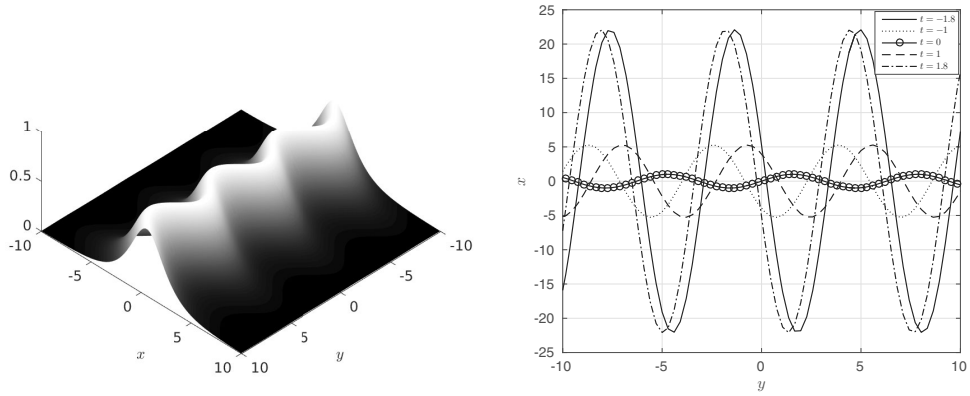

(a) (b)

Fig. 3. $|q^{[1]}|$ (44) with $\delta_1 = 0$, $\delta_1 = 0$, $\alpha_1 = 2/3$, $\beta_1 = 1/3$, $\eta_1 = -1/3$, $\xi_1 = 1/2$: 3D map at $t = 0$ (a), trajectories (45) (b).

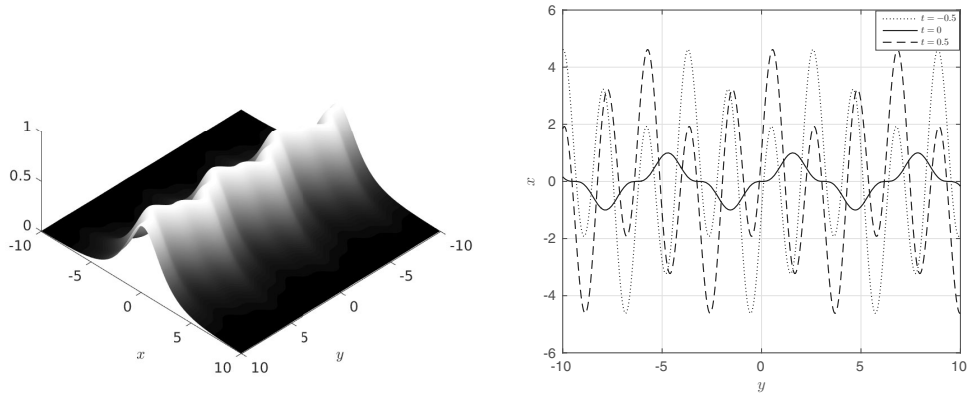

(a) (b)

Fig. 4. $|q^{[1]}|$ (46) with $\delta_1 = 0$, $\alpha_1 = 2/3$, $\beta_1 = 1/3$, $\eta_1 = -1/3$, $\xi_1 = 1/2$: 3D figure at $t = 0$ (a), trajectories (47) (b).

$f(y + 4\lambda^2 t)$ as a smooth function, we obtained order-n deformed soliton solutions.

Then we focused on the order-1 deformed soliton $q^{[1]}$, and discussed three kinds of deformed solitons in Section 3. Here is the summary of our findings:

- If $f_1 = \mu_1(y + 4\lambda_1^2 t)^m$, the solution $|q^{[1]}|$ is a polynomial one. The amplitude of $|q^{[1]}|$ is $2\beta_1$, and the trajectory is a polynomial function over time on the (x, y)-plane. Especially, if $m = 2$, it is a parabolic soliton with the velocity $(128\alpha_1^2\beta_1\eta_1 t, -4(\alpha_1^2 - \beta_1^2))$ on the (x, y)-plane, while in the case when $m = 3$, it is a cubic soliton with the velocity $(-1536\alpha_1^3\beta_1^2\eta_1 t^2, -4(\alpha_1^2 - \beta_1^2))$.
- If $f_1 = \mu_1 \sin^m(y + 4\lambda_1^2 t)$, the solution $|q^{[1]}|$ is a trigonometric one. The amplitude of $|q^{[1]}|$ is $2\beta_1$ and its trajectory is a trigonometric function over time on the (x, y)-plane. Especially, in the case when $m = 1$, the trajectory is a carrier wave and the velocity is $(8\alpha_1\xi_1 \cosh(8\alpha_1\beta_1 t), -4(\alpha_1^2 - \beta_1^2))$ on the (x, y)-plane, while in the case $m = 3$, the trajectory is a modulating wave, and the velocity is $(-24\alpha_1\xi_1 \cosh(8\alpha_1\beta_1 t)\sinh^2(8\alpha_1\beta_1 t), -4(\alpha_1^2 - \beta_1^2))$.
- If $f_1 = \mu_1(y + 4\lambda_1^2 t)^m$, the solution $|q^{[1]}|$ is a hyperbolic one. The amplitude of $|q^{[1]}|$ is $2\beta_1$ and its trajectory is a hyperbolic function over time on the (x, y)-plane. Especially, in the case when $m = 1$, the velocity is $(8\alpha_1\xi_1 \cos(8\alpha_1\beta_1 t), -4(\alpha_1^2 - \beta_1^2))$ on the (x, y)-plane, while in the case when $m = 3$, the velocity is $(8\alpha_1\xi_1 \sin(16\alpha_1\beta_1 t), -4(\alpha_1^2 - \beta_1^2))$.

We gave the formulas of the order-1 deformed soliton about arbitrary $f_1(y + 4\lambda_1^2 t)$, and the trajectory is $x = (f_1 + f_2 + 2\delta_1)/i(\lambda_1 - \lambda_2)$.

Besides, we gave the formulas and figures of the order-2 deformed soliton, and showed the evolutions of two samples over time in Section 4. It is interesting to study the interaction between two deformed solitons. We are going to do it in the near future.

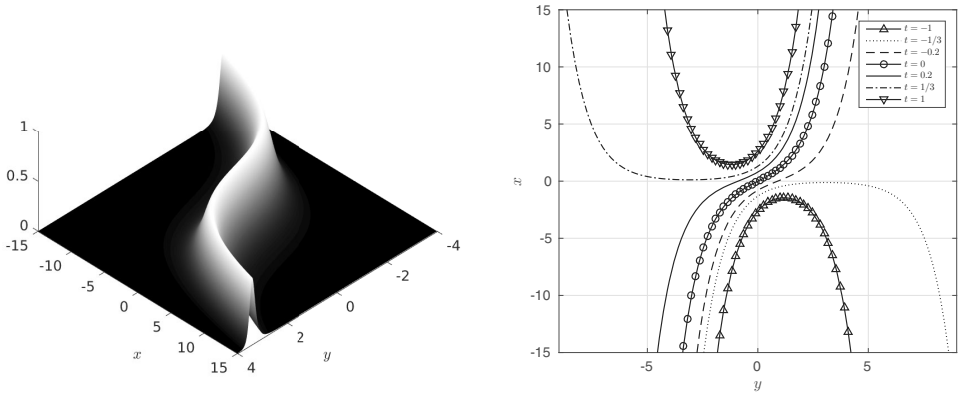

(a) (b)

Fig. 5. $|q^{[1]}|$ (50) with $\delta_1 = 0$, $\alpha_1 = 2/3$, $\beta_1 = 1/3$, $\eta_1 = -1/3$, $\xi_1 = 1/2$: 3D map at $t = 0$ (a), trajectories (51) (b).

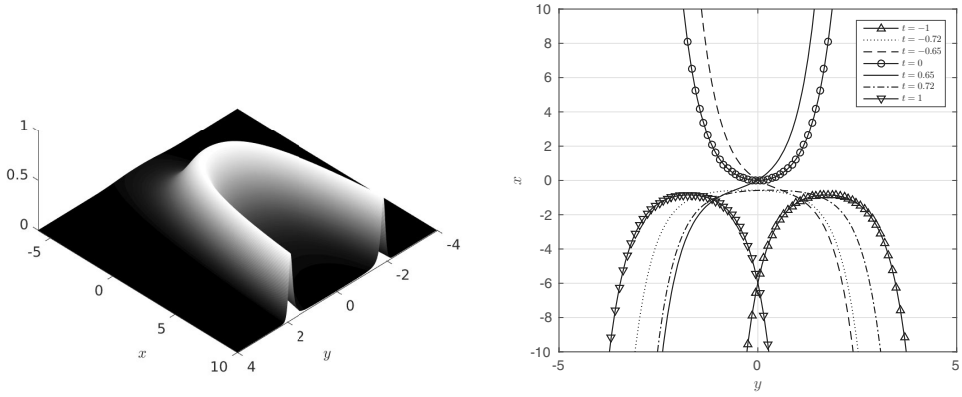

(a) (b)

Fig. 6. $|q^{[1]}|$ (52) with $\delta_1 = 0$, $\alpha_1 = 2/3$, $\beta_1 = 1/3$, $\eta_1 = -1/3$, $\xi_1 = 1/2$: 3D figure at $t = 0$ (a), trajectories (53)(b).

Acknowledgment

The authors want to thank all the referees who have provided constructive suggestions to help us improve the paper. This work is supported by the National Natural Science Foundation of China under the grants no. 11671219, 11871446, and 11805203.

References

Ablowitz, M.J., Ablowitz, M.A., Clarkson, P.A. and Clarkson, P.A. (1991). *Solitons, Nonlinear Evolution Equations and Inverse Scattering*, Cambridge University Press, Cambridge.

Biondini, G. (2007). Line soliton interactions of the Kadomtsev–Petviashvili equation, *Physical Review Letters* **99**(6): 064103.

Dai, C.Q., Zhu, S.Q., Wang, L.L. and Zhang, J.F. (2010). Exact spatial similaritons for the generalized (2+1)-dimensional nonlinear Schrödinger equation with distributed coefficients, *EPL (Europhysics Letters)* **92**(2): 24005.

El-Tantawy, S.A. and Moslem, W.M. (2014). Nonlinear structures of the Korteweg–de Vries and modified Korteweg–de Vries equations in non-Maxwellian electron-positron-ion plasma: Solitons collision and rogue waves, *Physics of Plasmas* **21**(5): 052112.

Erbay, H.A. (1998). Nonlinear transverse waves in a generalized elastic solid and the complex modified Korteweg–de Vries equation, *Physica Scripta* **58**(1): 9.

Erbay, S. and Şuhubi, E.S. (1989). Nonlinear wave propagation in micropolar media. II: Special cases, solitary waves and Painlevé analysis, *International Journal of Engineering Science* **27**(8): 915–919.

Gorbacheva, O.B. and Ostrovsky, L.A. (1983). Nonlinear vector waves in a mechanical model of a molecular chain, *Physica D: Nonlinear Phenomena* **8**(1–2): 223–228.

He, J.S., Tao, Y.S., Porsezian, K. and Fokas, A.S. (2013). Rogue wave management in an inhomogeneous nonlinear fibre with higher order effects, *Journal of Nonlinear Mathematical Physics* **20**(3): 407–419.

He, J.S., Wang, L.H., Li, L.J., Porsezian, K. and Erdélyi, R. (2014). Few-cycle optical rogue waves: Complex

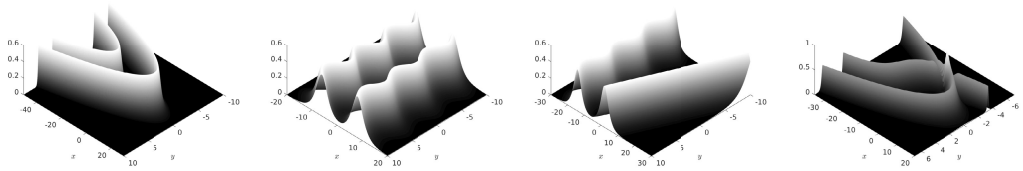

(a) (b) (c) (d)

Fig. 7. $|q^{[2]}|$ (59) with $\alpha_1 = 1/2$, $\beta_1 = 1/4$, $\alpha_2 = 3/5$, $\beta_2 = 1/4$, $\eta_1 = 1/3$, $\xi_1 = 1/3$, $\eta_2 = 1/2$, $\xi_2 = 2/3$, $t = 0$: $\delta_1 = -3, \delta_2 = 3$ (a), $\delta_1 = -1, \delta_2 = 1$ (b), $\delta_1 = -3, \delta_2 = 3$ (c), $\delta_1 = -2, \delta_2 = 3$ (d).

$$q^{[2]} = \frac{2i(\Theta_1 e^{-2\Gamma_1} + \Theta_2 e^{-2\Gamma_2} + \Theta_3 e^{2\Gamma_1} + \Theta_4 e^{2\Gamma_2}) + 2(\Theta_5 e^{-2\Gamma_1} + \Theta_6 e^{-2\Gamma_2} + \Theta_7 e^{2\Gamma_1} + \Theta_8 e^{2\Gamma_2})}{\sigma_1 \cosh(2\Gamma_1 + 2\Gamma_2) + \sigma_2 \cosh(2\Gamma_1 - 2\Gamma_2) - 4\beta_1\beta_2 \cos(2\Lambda_1 - 2\Lambda_2)}, \tag{57}$$

$$\begin{aligned}
\Theta_1 &= 2\beta_1\beta_2 \cos(2\Lambda_2) - \beta_2((\alpha_1 - \alpha_2)^2 - \beta_1^2 + \beta_2^2) \sin(2\Gamma_2),\\
\Theta_2 &= -2\beta_1\beta_2 \cos(2\Lambda_1) - \beta_1((\alpha_1 - \alpha_2)^2 + \beta_1^2 - \beta_2^2) \sin(2\Gamma_1),\\
\Theta_3 &= -2\beta_1\beta_2 \cos(2\Lambda_2) - \beta_2((\alpha_1 - \alpha_2)^2 - \beta_1^2 + \beta_2^2) \sin(2\Gamma_2),\\
\Theta_4 &= 2\beta_1\beta_2 \cos(2\Lambda_1) - \beta_1((\alpha_1 - \alpha_2)^2 + \beta_1^2 - \beta_2^2) \sin(2\Gamma_1),\\
\Theta_5 &= -2\beta_1\beta_2 \sin(2\Lambda_2) - \beta_2((\alpha_1 - \alpha_2)^2 - \beta_1^2 + \beta_2^2) \cos(2\Gamma_2),\\
\Theta_6 &= 2\beta_1\beta_2 \sin(2\Lambda_1) - \beta_1((\alpha_1 - \alpha_2)^2 + \beta_1^2 - \beta_2^2) \cos(2\Gamma_1),\\
\Theta_7 &= 2\beta_1\beta_2 \sin(2\Lambda_2) - \beta_2((\alpha_1 - \alpha_2)^2 - \beta_1^2 + \beta_2^2) \cos(2\Gamma_2),\\
\Theta_8 &= -2\beta_1\beta_2 \sin(2\Lambda_1) - \beta_1((\alpha_1 - \alpha_2)^2 + \beta_1^2 - \beta_2^2) \cos(2\Gamma_1),\\
\sigma_1 &= ((\alpha_1 - \alpha_2)^2 + (\beta_1 - \beta_2)^2), \quad \sigma_2 = (\alpha_1 - \alpha_2)^2 + (\beta_1 + \beta_2)^2,
\end{aligned} \tag{58}$$

$$\begin{aligned}
\Lambda_1 &= Re(-i\lambda_1 x + f_1 + \delta_1),\\
\Lambda_2 &= Re(-i\lambda_3 x + f_3 + \delta_2),\\
\Gamma_1 &= Im(-i\lambda_1 x + f_1 + \delta_1),\\
\Gamma_2 &= Im(-i\lambda_3 x + f_3 + \delta_2).
\end{aligned}$$

$$|q^{[2]}| = \frac{2\sqrt{(\Theta_1 e^{-2\Gamma_1} + \Theta_2 e^{-2\Gamma_2} + \Theta_3 e^{2\Gamma_1} + \Theta_4 e^{2\Gamma_2})^2 + (\Theta_5 e^{-2\Gamma_1} + \Theta_6 e^{-2\Gamma_2} + \Theta_7 e^{2\Gamma_1} + \Theta_8 e^{2\Gamma_2})^2}}{\sigma_1 \cosh(2\Gamma_1 + 2\Gamma_2) + \sigma_2 \cosh(2\Gamma_1 - 2\Gamma_2) - 4\beta_1\beta_2 \cos(2\Lambda_1 - 2\Lambda_2)}. \tag{59}$$

modified Korteweg–de Vries equation, *Physical Review E* **89**(6): 062917.

Hirota, R. (1972). Exact solution of the modified Korteweg–de Vries equation for multiple collisions of solitons, *Journal of the Physical Society of Japan* **33**(5): 1456–1458.

Kao, C.Y. and Kodama, Y. (2012). Numerical study of the KP equation for non-periodic waves, *Mathematics and Computers in Simulation* **82**(7): 1185–1218.

Karney, C.F.F., Sen, A. and Chu, F.Y.F. (1979). Nonlinear evolution of lower hybrid waves, *The Physics of Fluids* **22**(5): 940–952.

Khater, A.H., El-Kalaawy, O.H. and Callebaut, D.K. (1998). Bäcklund transformations and exact solutions for Alfvén solitons in a relativistic electron–positron plasma, *Physica Scripta* **58**(6): 545.

Kodama, Y., Oikawa, M. and Tsuji, H. (2009). Soliton solutions of the KP equation with V-shape initial waves, *Journal of Physics A: Mathematical and Theoretical* **42**(31): 312001.

Komatsu, T.S. and Sasa, S.-i. (1995). Kink soliton characterizing traffic congestion, *Physical Review E* **52**(5): 5574.

Korteweg, D.J. and de Vries, G. (1895). XLI. On the change of form of long waves advancing in a rectangular canal, and on a new type of long stationary waves, *The London, Edinburgh, and Dublin Philosophical Magazine and Journal of Science* **39**(240): 422.

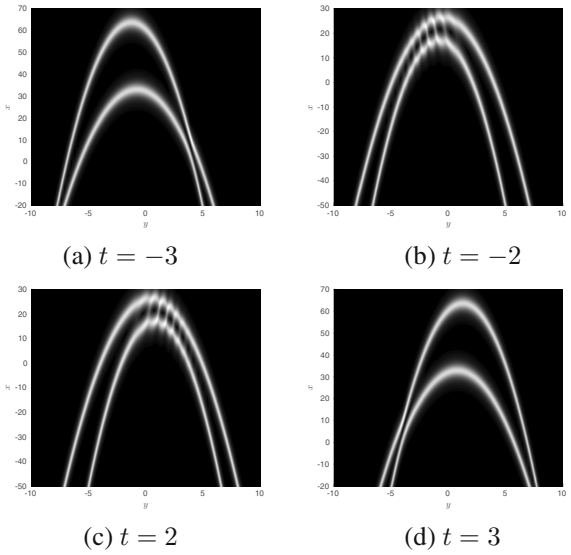

(a) $t = -3$ (b) $t = -2$

(c) $t = 2$ (d) $t = 3$

Fig. 8. Density figures of (57) with (58) and (60): $\alpha_1 = 1/2$, $\beta_1 = 1/4$, $\alpha_2 = 3/5$, $\beta_2 = 1/4$, $\eta_1 = 1/3$, $\xi_1 = 1/3$, $\eta_2 = 1/2$, $\xi_2 = 2/3$, $\delta_1 = -3, \delta_2 = 3$.

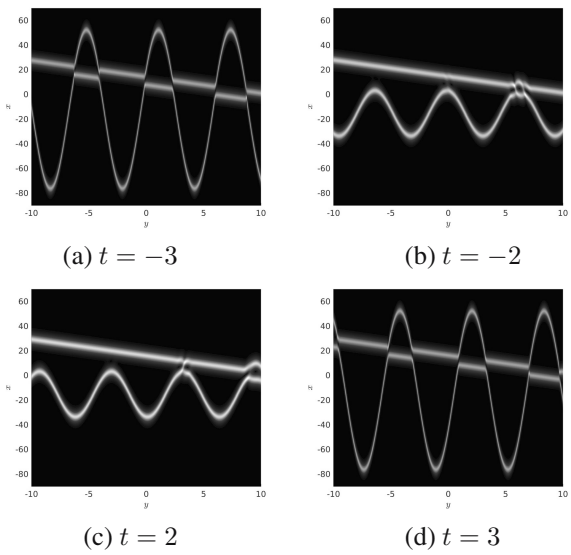

(a) $t = -3$ (b) $t = -2$

(c) $t = 2$ (d) $t = 3$

Fig. 9. Density figures of (57) with (58) and (61): $\alpha_1 = 1/2$, $\beta_1 = 1/4$, $\alpha_2 = 3/5$, $\beta_2 = 1/4$, $\eta_1 = 1/3$, $\xi_1 = 1/3$, $\eta_2 = 1/2$, $\xi_2 = 2/3$, $\delta_1 = -3, \delta_2 = 3$.

Kundu, A. (2008). Exact accelerating solitons in nonholonomic deformation of the KdV equation with a two-fold integrable hierarchy, *Journal of Physics A: Mathematical and Theoretical* **41**(49): 495201.

Li, Z.J., Hai, W.H. and Deng, Y. (2013). Nonautonomous deformed solitons in a Bose–Einstein condensate, *Chinese Physics B* **22**(9): 090505.

Liu, X.T., Yong, X.L., Huang, Y.H., Yu, R. and Gao, J.W. (2015). Deformed soliton, breather and rogue wave solutions of an inhomogeneous nonlinear Hirota equation, *Communications in Nonlinear Science and Numerical Simulation* **29**(1–3): 257–266.

Lonngren, K. E. (1998). Ion acoustic soliton experiments in a plasma, *Optical and Quantum Electronics* **30**(7–10): 615–630.

Lü, X., Zhu, H. W. Meng, X.H.Y.Z.C. and Tian, B. (2007). Soliton solutions and a Bäcklund transformation for a generalized nonlinear Schrödinger equation with variable coefficients from optical fiber communications, *Journal of Mathematical Analysis and Applications* **336**(2): 1305–1315.

Mollenauer, L.F., Stolen, R.H. and Gordon, J.P. (1980). Experimental observation of picosecond pulse narrowing and solitons in optical fibers, *Physical Review Letters* **45**(13): 1095.

Myrzakulov, R., Mamyrbekova, G., Nugmanova, G. and Lakshmanan, M. (2015). Integrable (2+1)-dimensional spin models with self-consistent potentials, *Symmetry* **7**(3): 1352–1375.

Osman, M.S. and Wazwaz, A.M. (2018). An efficient algorithm to construct multi-soliton rational solutions of the (2+1)-dimensional KdV equation with variable coefficients, *Applied Mathematics and Computation* **321**: 282–289.

Pal, R., Kaur, H., Raju, T.S. and Kumar, C. (2017). Periodic and rational solutions of variable-coefficient modified Korteweg–de Vries equation, *Nonlinear Dynamics* **89**(1): 617–622.

Porsezian, K., Seenuvasakumaran, P. and Ganapathy, R. (2006). Optical solitons in some deformed MB and NLS–MB equations, *Physics Letters A* **348**(3–6): 233–243.

Russell, S.J. (1844). Report on waves, *14th Meeting of the British Association for the Advancement of Science, York, UK*, pp. 311–390.

Sun, Z.Y. Gao, Y.T.L.Y. and Yu, X. (2011). Soliton management for a variable-coefficient modified Korteweg–de Vries equation, *Physical Review E* **84**(2): 026606.

Tao, Y.S., He, J.S. and Porsezian, K. (2013). Deformed soliton, breather, and rogue wave solutions of an inhomogeneous nonlinear Schrödinger equation, *Chinese Physics B* **22**(7): 074210.

Wadati, M. (1972). The exact solution of the modified Korteweg–de Vries equation, *Journal of the Physical Society of Japan* **32**(6): 1681–1681.

Wadati, M. (2008). Construction of parity-time symmetric potential through the soliton theory, *Journal of the Physical Society of Japan* **77**(7): 074005.

Wadati, M. and Ohkuma, K. (1982). Multiple-pole solutions of the modified Korteweg–de Vries equation, *Journal of the Physical Society of Japan* **51**(6): 2029–2035.

Wu, H.X., Zeng, Y.B. and Fan, T.Y. (2008). Complexitons of the modified KdV equation by Darboux transformation, *Applied Mathematics and Computation* **196**(2): 501–510.

Xing, Q.X., Wang, L.H., Mihalache, D., Porsezian, K. and He, J.S. (2017a). Construction of rational solutions of the real modified Korteweg–de Vries equation from its periodic solutions, *Chaos: An Interdisciplinary Journal of Nonlinear Science* **27**(5): 053102.

Xing, Q.X., Wu, Z.W., Mihalache, D. and He, J.S. (2017b). Smooth positon solutions of the focusing modified Korteweg–de Vries equation, *Nonlinear Dynamics* **89**(4): 2299–2310.

Xu, T.X., Qiao, Z.J. and Li, Y. (2011). Darboux transformation and shock solitons for complex mKdV equation, *Pacific Journal of Applied Mathematics* **3**(1/2): 137.

Yan, J.L. and Zheng, L.H. (2017). Conservative finite volume element schemes for the complex modified Korteweg–de Vries equation, *International Journal of Applied Mathematics and Computer Science* **27**(3): 515–525. DOI:10.1515/amcs-2017-0036.

Yesmakhanova, K., Shaikhova, G., Bekova, G. and Myrzakulov, R. (2017). Darboux transformation and soliton solution for the (2+1)-dimensional complex modified Korteweg–de Vries equations, *Journal of Physics: Conference Series* **936**: 012045.

Zabusky, N.J. and Kruskal, M.D. (1965). Interaction of solitons in a collisionless plasma and the recurrence of initial states, *Physical Review Letters* **15**(6): 240.

Zha, Q.L. and Li, Z.B. (2008). Darboux transformation and multi-solitons for complex mKdV equation, *Chinese Physics Letters* **25**(1): 8.

Zhang, H.Q. Tian, B.L.L.L. and Xue, Y.S. (2009). Darboux transformation and soliton solutions for the (2+1)-dimensional nonlinear Schrödinger hierarchy with symbolic computation, *Physica A: Statistical Mechanics and Its Applications* **388**(1): 9–20.

Zhang, Y.S., Guo, L.J., Chabchoub, A. and He, J.S. (2017). Higher-order rogue wave dynamics for a derivative nonlinear Schrödinger equation, *Romanian Journal of Physics* **62**: 102.

Zhang, Y.S., Guo, L.J., He, J.S. and Zhou, Z.X. (2015). Darboux transformation of the second-type derivative nonlinear Schrödinger equation, *Letters in Mathematical Physics* **105**(6): 853–891.

Feng Yuan is a doctoral candidate studying at the University of Science and Technology of China. Her major is mathematical physics, and her main research fields are nonlinear waves and integrable systems. She has published several articles in the area of exact solutions for nonlinear evolution equations.

Xiaoming Zhu is a doctoral candidate studying at the University of Science and Technology of China. His major is mathematical physics, and his main research fields are solitons and integrable systems.

Yulei Wang holds a PhD degree in plasma physics from the University of Science and Technology of China. His research interests include structure-preserving algorithms, applications of soliton theory in nonlinear plasma processes, runaway electron dynamics in magnetic confined fusion devices, and large-scale numerical simulations on high-performance computers.

Received: 15 November 2019
Revised: 23 December 2019
Re-revised: 17 January 2020
Accepted: 30 January 2020